General Robot Kinematics Decomposition without Intermediate Markers

Stefan Ulbrich*, Vicente Ruiz de Angulo†, Tamim Asfour*, Carme Torras† and Rüdiger Dillmann*
*Institute for Anthropomatics,
Karlsruhe Institute of Technology, Germany
Email: [stefan.ulbrich,tamim.asfour,dillmann]@kit.edu
† Institut de Robòtica i Informàtica Industrial,
CSIC-UPC, Barcelona
Email: [ruiz,torras]@iri.upc.edu

***Abstract*—The calibration of serial manipulators with high numbers of degrees of freedom by means of machine learning is a complex and time-consuming task. With the help of a simple trick this complexity can be drastically reduced and the speed of the learning procedure can be increased: When the robot is virtually divided into shorter kinematic chains, these subchains can be learned separately and, hence, much more efficiently than the complete kinematics. Such decompositions, however, require either the possibility to capture the poses of all end-effectors of all subchains at the same time, or they are limited to robots that fulfill special constraints. In this work, an alternative decomposition is presented that does not suffer from these limitations. An offline training algorithm is provided in which the composite subchains are learned sequentially with dedicated movements. A second training scheme is provided to train composite chains simultaneously and online. Both schemes can be used together with many machine learning algorithms. In the experiments, a PSOM algorithm modified for online learning was chosen to show the correctness of the approach.**

I. Introduction

With higher numbers of degrees of freedom (DoF) the calibration of serial manipulators (e.g., *anthropomorphic* manipulators) becomes increasingly complex and expensive [1]. In such systems, the need for calibration arises more often either due to deformations or—much more interestingly—because of reconfigurations such as tool-use. Instead of the costly traditional calibration routines, machine learning techniques can be used to learn the correlation between the joint angle configuration and the spatial pose of the end-effector, the *forward kinematics (FK)*. Usually, learning is accomplished by observing examples of input/output pairs of valid FK configurations. Many suitable learning algorithms have been proposed for this task. Among them there are the continuous extension of Kohonen maps, the *Parameterized Self Organizing Maps (PSOM)* [2], and *Locally Weighted Projection Regression (LWPR)* [3]. However, no learning algorithm can avoid the exponential growth ($\mathcal{O}(e^n)$) in the number n of DoF required to represent directly the FK with enough accuracy ([4] and [5]). This was the motivation for this work since the number of movements required in our humanoid robot [6] was impractical, even using state-of-the-art methods to learn FK. An effective way to palliate this problem are *decomposition* techniques [4][7]. Hereby, the robot is virtually divided into two (or more) subchains with fewer DoF each. These subchains can be learned much more efficiently than the complete chain; and the number of required training samples can be reduced to about its square root $\mathcal{O}(e^{\frac{n}{2}})$. The decomposition is known to work with many different learning systems.

Current techniques of learning by decomposition, however, have shortcomings. In [4], a decomposition is proposed that can be easily applied to robot manipulators whose last three axes intersect in a single point. This constraint excludes many possible robot architectures and may not hold anymore after a manipulator has suffered a deformation. A second approach that is general w.r.t. the choice of the robot architecture has been presented in [7]. However, it requires the ability to observe the spatial pose of all subchains' end-effectors at the same time in order to be able to learn. While this may be perfectly appropriate in setups with external cameras, the higher sensorial demand may exclude robots that learn from pure self-observation as it is the case of many humanoid robots.

This work presents a third option that is general w.r.t. the robot architecture and requires only the visibility of the original end-effector, at the expense of a more complex learning scheme. A batch algorithm well-suited for initial learning requires that, during the training of one subchain, the other subchains remain unchanged. This way, enough information can be gathered without the need to know the location of the individual subchains' end-effectors or origins, respectively. After an initial training, the decomposed kinematics can adapt online to many deformations such as a shift in the joint encoders or reconfigurations when using a tool. In contrast to the initial batch learning, this *online learning* allows for simultaneous movements of all subchains and it can be used during the operation of the robot.

In the experiments, these principles are validated using the new decomposition in conjunction with the PSOM learning

The work described in this paper was partially conducted within the EU Cognitive Systems projects PACO-PLUS (FP6-027657) and GRASP (FP7-215821) funded by the European Commission.

V. Ruiz de Angulo acknowledges support from Spanish Ministry of Science and Education, under the project DPI2007-60858.

C. Torras acknowledges support from the EU project Garnics (FP7-ICT-247947), the Consolider project MIPRCV (CSD2007-00018), and the Generalitat de Catalunya through the Robotics group (SGR2009-00155).

system. While PSOM originally does not offer online learning, it has proved possible to apply the Widrow-Hoff rule (also known as δ-rule) to the weights of this artificial neural network.

In the following two sections, the principles of the new proposed decomposition and the composition of the separately learned functions will be explained, respectively. The next section presents both the batch and the online learning algorithms. The document concludes with experiments and an outlook on future work.

II. Kinematics Decomposition

The proposed decomposition approach consists in using two kinematics functions that depend on disjoint subsets of the joint values. In Fig. 1, an example of the functions is provided for a robot with four rotational degrees of freedom.

We partition the joint variables $\boldsymbol{\theta} = (\theta_1, \theta_2 ... \theta_n)$ into two subsets $\boldsymbol{\zeta} = (\zeta_1, \zeta_2, ..., \zeta_k) := (\theta_1, \theta_2 ... \theta_k)$ and $\boldsymbol{\mu} = (\mu_1, .., \mu_{n-k}) := (\theta_{k+1}, ... \theta_n)$, that is, $\boldsymbol{\zeta}$ is the set of the first k joints and $\boldsymbol{\mu}$ the final $n-k$ ones. Then the direct kinematics function of the robot $K(\boldsymbol{\theta})$ (or $K(\boldsymbol{\zeta}, \boldsymbol{\mu})$ for convenience)[1] can be expressed as

$$K(\boldsymbol{\theta}) = K(\boldsymbol{\zeta}, \boldsymbol{\mu}) = K_{\boldsymbol{\zeta}}(\boldsymbol{\zeta}) \cdot K_{\boldsymbol{\mu}}(\boldsymbol{\mu}), \tag{1}$$

where $K_{\boldsymbol{\zeta}}$ and $K_{\boldsymbol{\mu}}$ are the kinematics of the two subchains of the robot implicitly defined by $\boldsymbol{\zeta}$ and $\boldsymbol{\mu}$, respectively.

The first function in the decomposition is

$$K_1(\boldsymbol{\zeta}; \tilde{\boldsymbol{\mu}}) := K(\boldsymbol{\zeta}, \tilde{\boldsymbol{\mu}}), \tag{2}$$

where $\tilde{\boldsymbol{\mu}}$ is an arbitrarily fixed value for $\boldsymbol{\mu}$. In the following, we will omit the parameter $\tilde{\boldsymbol{\mu}}$ from K_1 if not required. This function can then be reformulated as

$$K_1(\boldsymbol{\zeta}) = K_{\boldsymbol{\zeta}}(\boldsymbol{\zeta}) \cdot K_{\boldsymbol{\mu}}(\tilde{\boldsymbol{\mu}}) = K_{\boldsymbol{\zeta}}(\boldsymbol{\zeta}) \cdot C_{\tilde{\boldsymbol{\mu}}}, \tag{3}$$

where $C_{\tilde{\boldsymbol{\mu}}}$ is a constant transformation matrix associated to $\tilde{\boldsymbol{\mu}}$.

The second function, $K_2(\boldsymbol{\mu}; \tilde{\boldsymbol{\mu}})$, is the one that transforms $K(\boldsymbol{\zeta}, \tilde{\boldsymbol{\mu}})$ to $K(\boldsymbol{\zeta}, \boldsymbol{\mu})$, that is, it satisfies

$$K(\boldsymbol{\zeta}, \boldsymbol{\mu}) = K(\boldsymbol{\zeta}, \tilde{\boldsymbol{\mu}}) \cdot K_2(\boldsymbol{\mu}; \tilde{\boldsymbol{\mu}}). \tag{4}$$

Again, we will omit the parameter $\tilde{\boldsymbol{\mu}}$ in K_2 unless it is strictly required. Using $K_1(\boldsymbol{\zeta}) = K(\boldsymbol{\zeta}, \tilde{\boldsymbol{\mu}})$ the above equation can be expressed as

$$K(\boldsymbol{\zeta}, \boldsymbol{\mu}) = K_1(\boldsymbol{\zeta}) \cdot K_2(\boldsymbol{\mu}). \tag{5}$$

It is easy to check that K_2 is independent of $\boldsymbol{\zeta}$. Solving for K_2,

$$K_2(\boldsymbol{\mu}) = K(\boldsymbol{\zeta}, \tilde{\boldsymbol{\mu}})^{-1} \cdot K(\boldsymbol{\zeta}, \boldsymbol{\mu}), \tag{6}$$

and developing K into the two component kinematics, one gets

$$\begin{aligned} K_2(\boldsymbol{\mu}) &:= (K_{\boldsymbol{\zeta}}(\boldsymbol{\zeta}) \cdot K_{\boldsymbol{\mu}}(\tilde{\boldsymbol{\mu}}))^{-1} \cdot K_{\boldsymbol{\zeta}}(\boldsymbol{\zeta}) \cdot K_{\boldsymbol{\mu}}(\boldsymbol{\mu}) \\ &= K_{\boldsymbol{\mu}}(\tilde{\boldsymbol{\mu}})^{-1} \cdot K_{\boldsymbol{\zeta}}(\boldsymbol{\zeta})^{-1} \cdot K_{\boldsymbol{\zeta}}(\boldsymbol{\zeta}) \cdot K_{\boldsymbol{\mu}}(\boldsymbol{\mu}) \\ &= C_{\tilde{\boldsymbol{\mu}}}^{-1} \cdot K_{\boldsymbol{\mu}}(\boldsymbol{\mu}). \end{aligned} \tag{7}$$

[1]All kinematic functions $K_{\square}\colon \mathbb{R}^n \rightarrow \mathrm{SE}(3)$ are defined as mappings from the joint space into the group of rigid motions, whose elements can be expressed by homogeneous transformation matrices, for instance, or dual quaternions. In this work, we have chosen to use homogeneous matrices.

Now, it is also clear that K_2 has the shape of a kinematics function with $n-k$ degrees of freedom. In the end, we come up with two functions that depend only on one of the two disjoint subsets of variables. We would like to inform the reader that, alternatively, there exists a complementary decomposition not commented in depth in this article[2].

III. Kinematics Composition

The forward kinematics (FK) is obtained from (5). $K_1(\boldsymbol{\zeta})$ and $K_2(\boldsymbol{\mu})$ will be approximated by two learning systems (e.g, neural networks) N_1 and N_2, respectively. Therefore the FK will be estimated with

$$N(\boldsymbol{\zeta}, \boldsymbol{\mu}) = N_1(\boldsymbol{\zeta}) \cdot N_2(\boldsymbol{\mu}). \tag{8}$$

Regarding the inverse kinematics (IK), given a desired pose T, the joint coordinates $\boldsymbol{\theta} = (\zeta_1, \ldots, \zeta_k, \mu_1, \ldots, \mu_{n-k})$ form a valid inverse kinematics solution iff

$$K(\boldsymbol{\zeta}, \boldsymbol{\mu}) = K_1(\boldsymbol{\zeta}) \cdot K_2(\boldsymbol{\mu}) = T, \tag{9}$$

which can be approximated with

$$N(\boldsymbol{\zeta}, \boldsymbol{\mu}) = N_1(\boldsymbol{\zeta}) \cdot N_2(\boldsymbol{\mu}) = T. \tag{10}$$

The constraint (9) can be rewritten in another form:

$$\begin{aligned} & K_{\boldsymbol{\zeta}}(\boldsymbol{\zeta}) \cdot C_{\tilde{\boldsymbol{\mu}}} \cdot C_{\tilde{\boldsymbol{\mu}}}^{-1} \cdot K_{\boldsymbol{\mu}}(\boldsymbol{\mu}) = T \\ \Leftrightarrow \quad & K_{\boldsymbol{\zeta}}(\boldsymbol{\zeta}) = T \cdot K_{\boldsymbol{\mu}}(\boldsymbol{\mu})^{-1}. \end{aligned} \tag{11}$$

where equations (3) and (7) have been used.

This is the same equality used in [7]: the first subchain of the robot must be the same as the last one reverted and transformed to the desired pose. As mentioned earlier, a limitation of this approach is that, in order to learn $K_{\boldsymbol{\zeta}}(\boldsymbol{\zeta})$ and $K_{\boldsymbol{\mu}}(\boldsymbol{\mu})^{-1}$, one needs to detect the pose of an intermediate marker placed in the k-th link. The advantage of (10) is that, although the underlying constraint is the same, the involved functions K_1 and K_2 can be learned by using only the ability to detect the end-effector pose (see next section).

There exist many ways to satisfy the constraint (10), most of them involving the Jacobian of $N(\boldsymbol{\zeta}, \boldsymbol{\mu})$ [8], [9], [10], [11]. This matrix is obtained by combining the partial derivatives of each network, N_1 and N_2, with the outputs of the other network according to (8):

$$\begin{aligned} & \tfrac{\partial}{\partial \zeta_i} N(\boldsymbol{\zeta}, \boldsymbol{\mu}) = \tfrac{\partial}{\partial \zeta_i} N_1(\boldsymbol{\zeta}) \cdot N_2(\boldsymbol{\mu}) \\ \text{and} \quad & \tfrac{\partial}{\partial \mu_j} N(\boldsymbol{\zeta}, \boldsymbol{\mu}) = N_1(\boldsymbol{\zeta}) \cdot \tfrac{\partial}{\partial \mu_j} N_2(\boldsymbol{\mu}). \end{aligned} \tag{12}$$

IV. Learning

The learning of $K_1(\boldsymbol{\zeta})$ and $K_2(\boldsymbol{\mu})$ can be accomplished with strategies entailing different degrees of parallelism and sophistication. We show the two main ones below. It is important to point out that, in every case, we only require the ability to sense the pose of the end-effector in the chosen configuration $K(\boldsymbol{\zeta}, \boldsymbol{\mu})$.

[2]The alternative decomposition is $L_1(\boldsymbol{\mu}) = K(\tilde{\boldsymbol{\zeta}}, \boldsymbol{\mu})$, $L_2(\boldsymbol{\zeta}) = K(\boldsymbol{\zeta}, \boldsymbol{\mu}) \cdot L_1(\boldsymbol{\mu})^{-1}$. The kinematics composition is obtained from L_2 definition, $K(\boldsymbol{\zeta}, \boldsymbol{\mu}) = L_2(\boldsymbol{\zeta}) L_1(\boldsymbol{\mu})$.

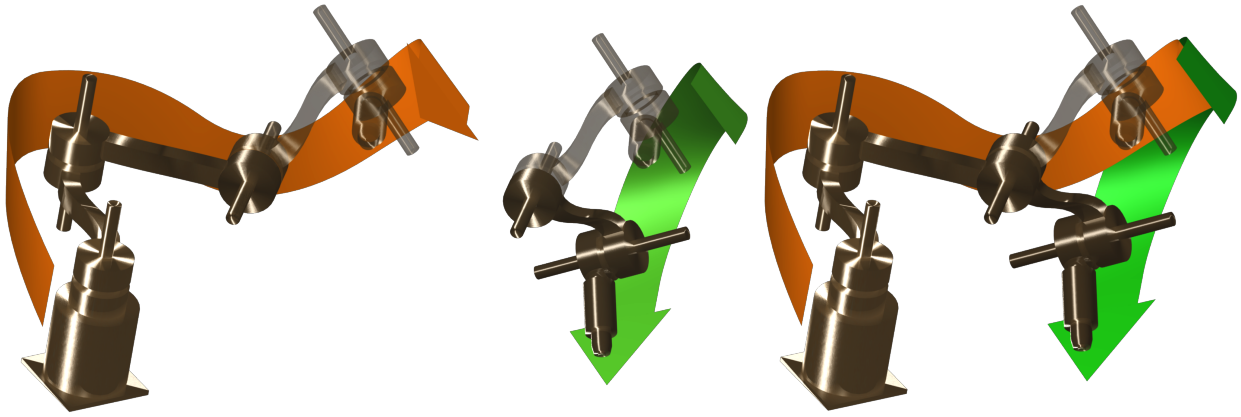

(a) $K_1(\boldsymbol{\zeta}) = K_\zeta(\boldsymbol{\zeta}) \cdot C_{\tilde{\boldsymbol{\mu}}}$ (b) $K_2(\boldsymbol{\mu}) = C_{\tilde{\boldsymbol{\mu}}}^{-1} \cdot K_\mu(\boldsymbol{\mu})$ (c) $K(\boldsymbol{\zeta}, \boldsymbol{\mu}) = K_1(\boldsymbol{\zeta}) \cdot K_2(\boldsymbol{\mu})$

Fig. 1. Example of the decomposition for a robot with four rotational degrees of freedom. The first kinematics function K_1 is shown in (a). It is the transformation from the robot base to its end-effector when the last (two) degrees of freedom are assigned to constant values (namely $\tilde{\boldsymbol{\mu}}$). The constant part of the robot is called $C_{\tilde{\boldsymbol{\mu}}}^{-1}$ (see (3)). This part of the robot is rendered transparently in this image. During learning, the end-effector frame is tracked while moving the first two axes. The second kinematics function shown in (b) is K_2. This function is a composition of the last half of the robot (i.e., K_μ) with two active joints and $C_{\tilde{\boldsymbol{\mu}}}$ (see (7)) which is, again, displayed transparently. That is, K_2 is the transformation from the tail of K_1 to the real end-effector frame. When learning this function, the real end-effector (opaque) is tracked while the first two joints are fixed to the reference values in $\tilde{\boldsymbol{\zeta}}$. Consequently, as shown in (c), the combination of K_1 and K_2 results in the complete robot transformation.

1) Independent learning: The simplest approach is to learn each function independently in a phase preceding the functional operation of the robot. The learning of K_1 and K_2, shown in Algorithms 1 and 2, proceeds sequentially. Algorithm 1 moves the first joints $\boldsymbol{\zeta}$ to random values while fixing $\boldsymbol{\mu}$ to a reference value. In Algorithm 2, a little trick is used to learn K_2. Normally, one should select an input $\boldsymbol{\mu}_i$ and then move to $K(\boldsymbol{\zeta}_i, \boldsymbol{\mu}_i)$ and $K(\boldsymbol{\zeta}_i, \tilde{\boldsymbol{\mu}})$ to obtain the desired output

$$K(\boldsymbol{\zeta}_i, \tilde{\boldsymbol{\mu}})^{-1} \cdot K(\boldsymbol{\zeta}_i, \boldsymbol{\mu}_i),$$

where $\boldsymbol{\zeta}_i$ is arbitrary in each iteration. But if $\boldsymbol{\zeta}_i$ remains always the same, $K(\boldsymbol{\zeta}_i, \tilde{\boldsymbol{\mu}})^{-1}$ is a constant that can be obtained before the loop, and one movement is saved in each iteration. In short, both Algorithms 1 and 2 consist basically in fixing some joints and moving the remaining ones.

There are many possible variations of Algorithm 2. If $\boldsymbol{\mu}$ is constrained for some values of $\boldsymbol{\zeta}$ (e.g., in order to keep the end-effector in the field of view), we can run Algorithm 2 several times with a different selection of $\hat{\boldsymbol{\zeta}}$. If the constraints require a different value of $\boldsymbol{\zeta}$ for each value of $\boldsymbol{\mu}_i$, it is still possible to learn K_2 with only one movement in each iteration. The selection of $\boldsymbol{\zeta}_i$ must be introduced in the loop (line 1 and 2 are removed), the movement must be performed to $(\boldsymbol{\zeta}_i, \boldsymbol{\mu}_i)$ and, finally, $N_1(\boldsymbol{\zeta}_i)^{-1}\ T_i$ must be used as output for N_2. This approximation follows from equation (10). The drawback is that these output data depend on an approximation of K_1. But since K_1 has a low dimensionality and it has been learned previously, the error introduced is negligible.

Algorithm 1: Learning of $K_1(\boldsymbol{\zeta})$.

1 **foreach** $\boldsymbol{\zeta}_i \in Training\_Set$ **do**
2 Move to $(\boldsymbol{\zeta}_i, \tilde{\boldsymbol{\mu}})$ and observe $T_i = K(\boldsymbol{\zeta}_i, \tilde{\boldsymbol{\mu}})$
3 Learn N_1 with $\boldsymbol{\zeta}_i$ as input and T_i as output.

Algorithm 2: Learning of $K_2(\boldsymbol{\mu})$.

1 Select $\hat{\boldsymbol{\zeta}}$
2 Move to $(\hat{\boldsymbol{\zeta}}, \tilde{\boldsymbol{\mu}})$ and observe $T_{\tilde{\boldsymbol{\mu}}} = K(\hat{\boldsymbol{\zeta}}, \tilde{\boldsymbol{\mu}})^{-1}$
3 **foreach** $\boldsymbol{\mu}_i \in Training\_Set$ **do**
4 Move to $(\hat{\boldsymbol{\zeta}}, \boldsymbol{\mu}_i)$ and observe $T_i = K(\hat{\boldsymbol{\zeta}}, \boldsymbol{\mu}_i)$
5 Learn N_2 with $\boldsymbol{\mu}_i$ as input and $T_{\tilde{\boldsymbol{\mu}}}\ T_i$ as output.

2) Concurrent learning: None of the learning strategies above can be used to perform on-line learning, that is, learning that is integrated in the normal working operation. The strategy that we present now parallelizes the learning of all the functions that compese the kinematic model. And, interestingly, it permits carrying out arbitrary movements as, for instance, those required by an application while, at the same time, refining the estimation of the robot kinematics.

In fact, equation (9) implicitly provides values for K_1, $(T \cdot K_2(\boldsymbol{\mu})^{-1})$, and for K_2, $(K_1(\boldsymbol{\zeta})^{-1} \cdot T)$, which depend on one another. It is possible to use their estimates N_1 and N_2 to obtain new training samples as it is shown in Algorithm 3.

Note that $\tilde{\boldsymbol{\mu}}$ is missing completely in Algorithm 3 and, thus, the algorithm can converge to functions with any value of $\tilde{\boldsymbol{\mu}}$. Moreover, the algorithm converges to whatever functions N_1 and N_2 satisfying

$$K(\boldsymbol{\zeta}, \boldsymbol{\mu}) = N_1(\boldsymbol{\zeta}) \cdot N_2(\boldsymbol{\mu}), \tag{13}$$

which, in general, would not have the shape of $K_1(\boldsymbol{\zeta}; \tilde{\boldsymbol{\mu}})$ and $K_2(\boldsymbol{\mu}; \tilde{\boldsymbol{\mu}})$ for any $\tilde{\boldsymbol{\mu}}$. But in Appendix A we show that, given an a priori fixed $\tilde{\boldsymbol{\mu}}$, after convergence N_1 and N_2 can be expressed as

$$N_1(\boldsymbol{\zeta}) = K_1(\boldsymbol{\zeta}; \tilde{\boldsymbol{\mu}})\ N_2(\tilde{\boldsymbol{\mu}})^{-1}, \tag{14}$$

$$N_2(\boldsymbol{\mu}) = N_2(\tilde{\boldsymbol{\mu}})\ K_2(\boldsymbol{\mu}; \tilde{\boldsymbol{\mu}}). \tag{15}$$

There is nothing wrong with these functions, since they constitute a valid composition. But it should be noted that N_1 and N_2 may change suddenly their values when switching from concurrent learning to independent learning. Anyway, a slight modification of Algorithms 1 and 2 would allow to learn the right parts of equations (14) and (15).

The fact that there are many functions yielding a valid kinematics decomposition has a potential advantage. N_1 (or N_2) alone can adapt to certain kinematic changes, absorbing the required changes for K_1 and K_2. This is interesting because learning only one function is much quicker than learning two interdependent functions. For example, if the kinematics of the robot undergoes a deformation equivalent to a linear transformation, that is,

$$K'(\boldsymbol{\zeta}, \boldsymbol{\mu}) = K(\boldsymbol{\zeta}, \boldsymbol{\mu}) \cdot P,$$

the system can be quickly adapted by only learning N_2, as shown in Appendix B. A linear transformation includes the rigid transformations involved in the adaptation to a tool and, also, some effects that result from a poorly calibrated camera such as a scaling of the sensor data.

Note that the learning of N_1 and N_2 is interdependent because, at each iteration, their corrections aim to reduce the same error quantity, $||N_1(\boldsymbol{\zeta}) \cdot N_2(\boldsymbol{\mu}) - T_i||$. To put the learning of N_1 and N_2 on an equal ground, in Algorithm 3 the desired outputs for both functions are calculated *before* any modification takes place. Anyway, special attention has to be payed to the learning rates used to learn N_1 and N_2. If, for instance, N_1 is corrected to make this error 0, a subsequent correction of N_2 of the same magnitude, will result in $N_1(\boldsymbol{\zeta}) \cdot N_2(\boldsymbol{\mu}) - T_i$ having a value opposite to the initial one, and the same error magnitude. Therefore, the learning rates should be such that, the correction of N_1 (or N_2) alone cancel out no more than half of the error or, in any case, the sum of the corrections to N_1 and N_2 must cancel out (partially or completely) $N_1(\boldsymbol{\zeta}) \cdot N_2(\boldsymbol{\mu}) - T_i$ without reverting its sign.

Algorithm 3: Simultaneous learning of $K_1(\boldsymbol{\zeta})$ and $K_2(\boldsymbol{\mu})$.

1 **foreach** $(\boldsymbol{\zeta}_i, \boldsymbol{\mu}_i) \in Training\_Set$ **do**
2 Move to $(\boldsymbol{\zeta}_i, \boldsymbol{\mu}_i)$ and observe $T_i = K(\boldsymbol{\zeta}_i, \boldsymbol{\mu}_i)$
3 Set $T_{i,1} := T_i \cdot N_2(\boldsymbol{\mu}_i)^{-1}$ and $T_{i,2} := N_1(\boldsymbol{\zeta}_i)^{-1} \cdot T_i$
4 Learn N_1 with $\boldsymbol{\zeta}_i$ as input and $T_{i,1}$ as output.
5 Learn N_2 with $\boldsymbol{\mu}_i$ as input and $T_{i,2}$ as output.

V. Experiments

We use two simulated robots having eight active DoF, in the offline learning experiment, and five in the online learning experiments. The Denavit-Hartenberg parameters of these robots are equal for each segment i, namely $\alpha_i = 90°$, $a_i = 200\,\mathrm{mm}$ and $d_i = 0\,\mathrm{mm}$. This results in arm lengths of $1600\,\mathrm{mm}$ and $1000\,\mathrm{mm}$ at the rest positions. The samples used for training and testing are generated evaluating the FK in joint angles drawn from $[-45°, 45°]$. In all experiments, there are 1000 samples in the test sets that are generated randomly by sampling uniformly angles from this range. The actual learning is done in all cases by PSOM networks. The orientations of the end-effector are expressed by means of rotation matrices. Each of these matrices' elements are learned independently by the PSOM algorithm. As a result the output may not always be a valid rotation matrix which can be critical when concatenating the individual networks' outputs. For this reason, a Gram-Schmidt orthonormalization is applied systematically to the rotational part of all networks to improve the output quality[3]. This includes also the orientation parts of N_1 and N_2 in line 3 of Algorithm 3. The calculus of the IK using the FK model will add a numerical error dependent on the algorithm used for this purpose. Because of this, all experiments in this paper focus on the evaluation of the accuracy of the FK representations.

A. Offline Learning

This experiment examines the offline learning as presented in Algorithms 1 and 2. The kinematics of a robot with eight independent and active degrees of freedom is learned by PSOM networks. The input values are fixed to the nodes of an eight-dimensional rectangular grid that encloses all possible joint angles of the training data. For learning, the output values of the forward kinematics at these joint positions are assigned to the corresponding neurons. Once learned, the PSOM interpolates between the learned pose values in order to estimate the forward kinematics. The number of neurons in each dimension of the grid was different in the PSOMs used in the experiment. They are indicated by the labels of selected data points (with a comma separating the grid dimensions of the two networks in the decomposition case) in Figs. 2, 3 and 4.

Fig. 2 shows the mean error on the test data in relation to the number of samples (i.e., neurons) on a logarithmic scale. In this graph, one can directly see that —for higher numbers of neurons— the curves are nearly parallel to each other. The curve of the decomposition lies roughly in the middle between the axis of abscissas and the curve for the single network. This indicates that, in order to get the same level of accuracy, in comparison to the single network, only the square root of the number of samples is required to train the decomposition networks. In Figs 3 and 4, the same relation is shown on a linear scale. The most interesting part is amplified and plotted in Fig. 4. The mean error on the training data of the decomposition drops much quicker as compared to the single network. This point of view emphasizes the advantage of the decomposition when applied to a robot system. Figure 5 shows how many samples are necessary to obtain a certain level of precision. In the diagram, the 95%-quantiles for the decomposition and the single networks are displayed, that is, the precision threshold below which lie 95% of the errors on the test data. Again, a reduction to nearly the square root of the required samples can be appreciated thanks to the logarithmic scale.

[3]Note that even if one is only interested in learning positions, the orientation part of N_1 and N_2 is also involved in the calculation of the position of the composite kinematics.

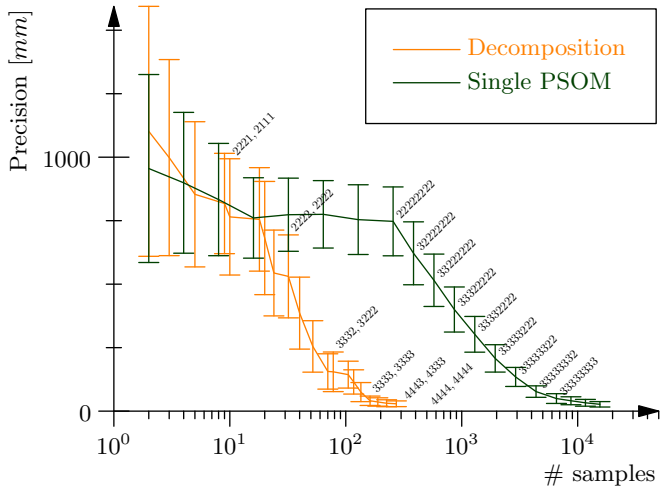

Fig. 2. Comparison of the offline learning using the decomposition and a single PSOM with different training samples and, consequently, different numbers numbers of neurons as indicated by the labels. The diagram uses a logarithmic scale and the standard deviation of the precision is included in form of error bars.

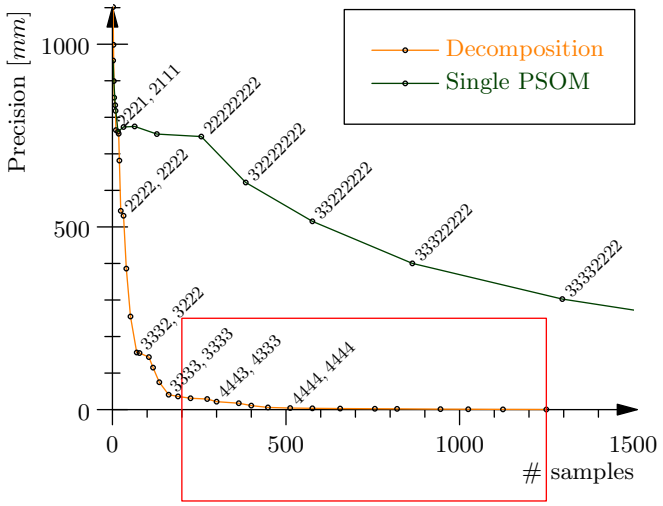

Fig. 3. Performance of the decomposition and a single PSOM when learning offline shown on a linear scale. In Fig. 4, The highlighted area is shown enlarged.

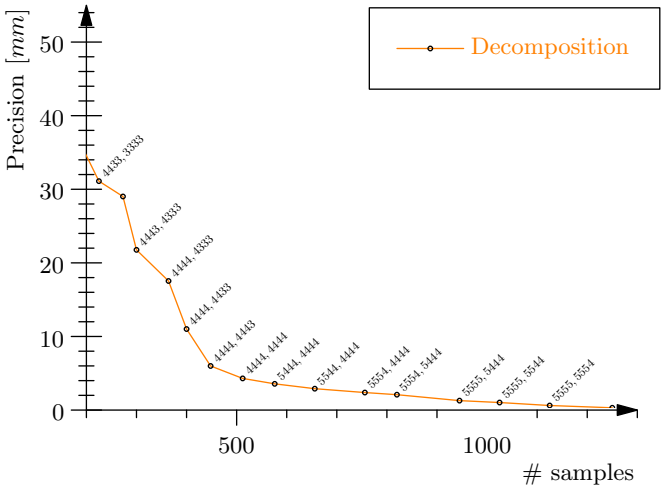

Fig. 4. Closeup showing the number of training samples needed to achieve a high precision on a robot with eight DoF.

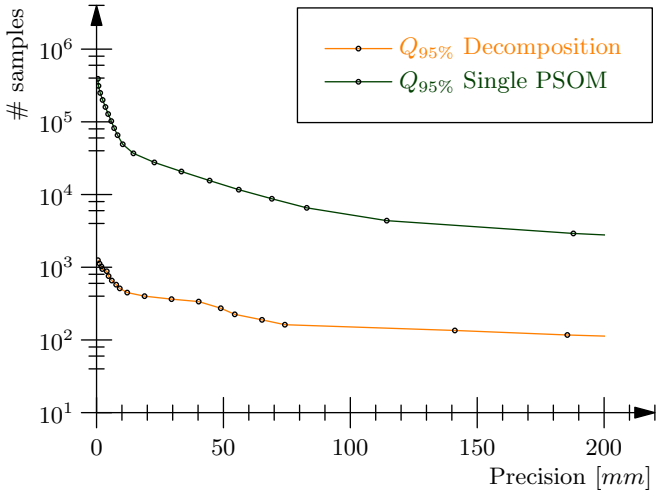

Fig. 5. Convergence of the decomposition and a single PSOMs for higher precision. On the logarithmic scale it can seen that, using the decomposition, the number of training samples required to obtain a given precision is roughly reduced to its square root.

B. Online Learning

Now we investigate how learning and the refinement of the decomposition can be performed during the normal operation of the robot using Algorithm 3. As the regular PSOM algorithm requires grid-organized data, it is not naturally suited for online learning. Here, we have carried out a grid-preserving supervised adaptation by updating part of the weight of the neurons according to the Widrow-Hoff rule or *normalized least mean squares (NLMS)* method (or δ-rule for single layer preceptrons):

$$w_{\boldsymbol{a}}^{t+1} = w_{\boldsymbol{a}}^{t} + \epsilon \cdot H_{\boldsymbol{a}}(\boldsymbol{a}, \boldsymbol{\theta}) \cdot (w_{\boldsymbol{a}}^{t} - \boldsymbol{x}), \tag{16}$$

where $w_{\boldsymbol{a}}^{t}$ is the weight subvector of the neuron at grid position $\boldsymbol{a}$ representing the robot pose, $\epsilon \in (0, 1]$ is the learning rate, and $(\boldsymbol{\theta}, \boldsymbol{x})$ is a sample input/output pair. If the learning rate ϵ in equation (16) equals one, the network adapts completely to the currently presented sample, that is, the output of the network then equals $\boldsymbol{x}$. According to the discussion at the end of Section IV-2, the learning rates for N_1 and N_2 have been set to 0.5, which adapts completely the combination of the two networks to the presented sample. In this way, the two networks cancel out the same amount of error.

This online learning initially adapts very fast to modifications of the kinematics. In the long term, however, this way of learning is much slower compared to offline learning, that is, a much higher number of samples is required to gain the same level of precision. For this reason, we have reduced the number of effective degrees of freedom to five in this experiment.

In this section, we investigate how the decomposition of a robot with five revolute joints adapts to two modifications that are likely to occur in real application. Training and test samples are generated with the modified robot by moving to random configurations with angles out of the same angular range as during the initial training (i.e., $[-45°, 45°]$). The refinement starts with initial models that are approximations of the intact robot FK consisting of a single PSOM with

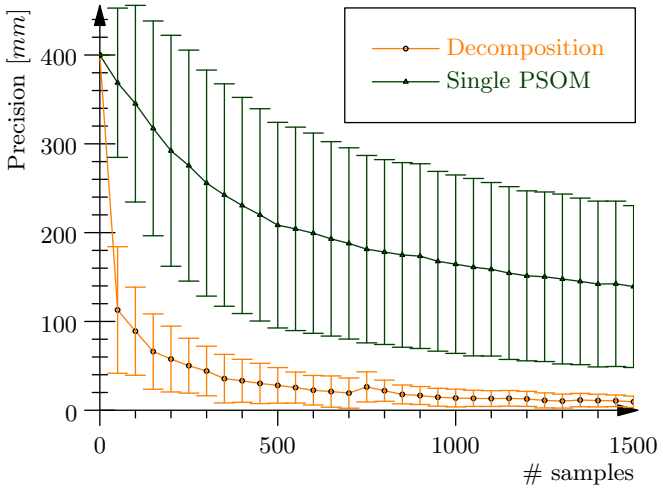

Fig. 6. Learning curves of the new incremental online learning algorithm after a deformation simulating tool use (last element extended 400 mm). Leaning begins from models of the original kinematics learned offline. The Standard deviations are shown as error bars.

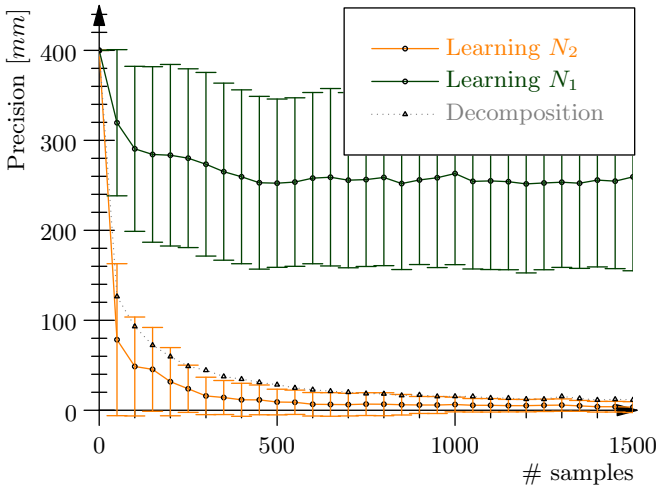

Fig. 7. This image shows the performance of learning only one of the networks in the decomposition after the same deformation as in Fig. 6).

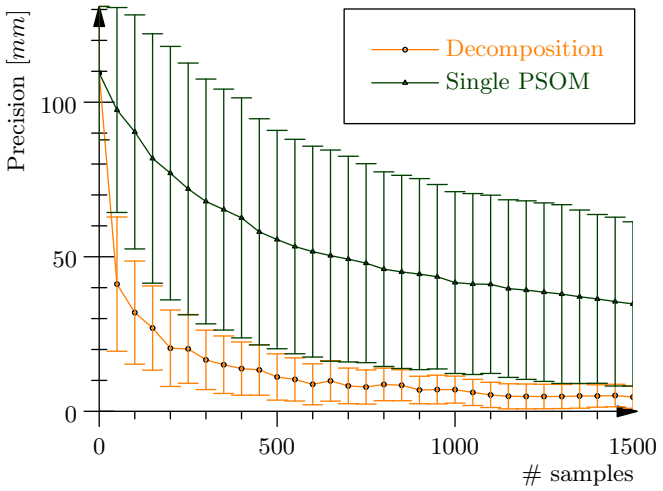

Fig. 8. Learning curves of the new incremental online learning algorithm when suddenly a constant of 10° is added to each angle.

$5^5 = 3125$ neurons and a decomposition with $5^3 + 5^2 = 150$ neurons.

The first modification of the kinematics is a translation of $400\,\mathrm{mm}$ applied to the end-effector in order to simulate tool use. Another kind of modification can occur with incremental encoders that require calibration upon each startup. We simulated a modification of this type, by adding a constant of 10° to all robot joints. The results of learning after these two deformations have taken place are presented in the diagrams in Fig. 6 and Fig. 8, respectively. In both diagrams, it can be immediately seen that the decomposition leads to better levels of accuracy much more quickly as compared to the single network. Note also that the error bars of the single PSOM curve remain in both figures almost constant, while in that of the decomposition they shrink notoriously. Adaptation for the first training samples is very fast and afterwards the curves converge to the optimal solution even though slowly. For the first deformation, we further investigated if learning can be accelerated by adapting only one of the individual networks N_1 and N_2 (see Fig. 7). One can see that only the second network N_2 is able to compensate the deformation and, as a matter of fact, it does significantly quicker than learning simultaneously both functions: the error reached after learning 500 samples with N_2 alone is lower than that obtained after adapting to learn 1500 samples both networks. Consequently, this learning strategy is useful to learn deformations known to be linear transformations of the original kinematics. The most prominent example in this context is tool-use.

VI. Conclusion

In this paper, we pointed out the importance of modeling kinematics functions by means of machine learning techniques. The main difficulty, hereby, lies in the fact that the number of training samples required to acquire an adequately accurate model grows exponentially with the number of degrees of freedom. Decomposition techniques have proved to be an effective means to solve this problem by reducing the amount of training samples to about its square root (in the case of one single decomposition). However, the decomposition schemes presented in previous works either impose restrictions to the kinematics (e.g., three intersecting axes) or require more parts of the robot to be visualized, increasing the demand for additional sensors.

This work presents a new strategy to learn a decomposition that overcomes these restrictions. The kinematic function is split up into two dependent sub-functions that can either be learned offline—one after another—or can be simultaneously refined in an incremental online learning process. The theoretical insights were verified using two simulated robots with eight and five active revolute degrees of freedom, respectively. We chose the parameterized self-organizing maps (PSOM) as the underlying machine learning algorithm and further enhanced it by incorporating a supervised incremental learning rule—namely the Hoff-Widrow rule. In a series of experiments, we demonstrated that the learning was sped up drastically (i.e., the number of required training samples was reduced to its square root) as predicted and we showed the relation between

learning speed and the resulting model precision. In further experiments, we showed that the decomposition can speed up enormously the convergence of the online refinement of initial models, for example in the case of tool-use or while recovering from a shift in the joint encoders. Altogether, the combination of both learning methods—creating an initial model, in simulation for instance, and refining it online afterwards—leads to a very efficient method to learn the complete kinematics of even very complex robots with many active degrees of freedom. The new decomposition is compatible with most of the algorithms devised to learn FK [12], [13], [14], and it can make the use of a learned FK affordable to those approaches using a known FK to obtain IK information [15], [16], [11]. Because of its greater simplicity and generality, the decomposition presented here clearly outperforms the approach in [4]. Instead, the comparison with [7] is more intrincate. If only offline learning is required, the new decomposition is again advantageous, since it offers the same results with less sensorial requirements. But, if these requirements can be easily fulfilled (thanks for example to external cameras), online learning is simpler and quicker in [7], because the learned functions are not interdependent. Extending the presented two-function decomposition to involve more than two functions (with less DoF) as in [7] is a feasible future work. Our future plains include the application of this decomposition technique to the ARMAR humanoid robot [6].

APPENDIX

A. Functions satisfying the decomposition

We will prove that all functions N_1, N_2 satisfying the composition equation (13) used in Algorithm 3, have the form

$$\begin{array}{rcl} N_1(\boldsymbol{\zeta}) & = & K_1(\boldsymbol{\zeta};\tilde{\boldsymbol{\mu}}) \cdot C^{-1} \\ N_2(\boldsymbol{\mu}) & = & C \cdot K_2(\boldsymbol{\mu};\tilde{\boldsymbol{\mu}}), \end{array} \tag{17}$$

where C is equal to $N_2(\tilde{\boldsymbol{\mu}})$.

First, we show that functions of the same form as (17) do in fact satisfy (13),

$$\begin{array}{rcl} N_1(\boldsymbol{\zeta}) \cdot N_2(\boldsymbol{\mu}) & = & K_1(\boldsymbol{\zeta};\tilde{\boldsymbol{\mu}}) \cdot C^{-1} \cdot C \cdot K_2(\boldsymbol{\mu};\tilde{\boldsymbol{\mu}}) \\ & = & K_1(\boldsymbol{\zeta};\tilde{\boldsymbol{\mu}}) \cdot K_2(\boldsymbol{\mu};\tilde{\boldsymbol{\mu}}) \\ & = & K(\boldsymbol{\zeta},\boldsymbol{\mu}), \end{array} \tag{18}$$

and that, given that form, C must equal $N_2(\tilde{\boldsymbol{\mu}})$:

$$N_2(\tilde{\boldsymbol{\mu}}) = C \cdot K_2(\tilde{\boldsymbol{\mu}};\tilde{\boldsymbol{\mu}}) = C \cdot I = C, \tag{19}$$

where I is the identity matrix. Now, we show that no form other than (17) is possible for N_1, N_2. We begin by defining the functions

$$\begin{array}{rcl} \epsilon_1(\boldsymbol{\zeta}) & \equiv & K_1(\boldsymbol{\zeta};\tilde{\boldsymbol{\mu}})^{-1} \cdot N_1(\boldsymbol{\zeta}) \\ \epsilon_2(\boldsymbol{\mu}) & \equiv & N_2(\boldsymbol{\mu}) \cdot K_2(\boldsymbol{\mu};\tilde{\boldsymbol{\mu}})^{-1}. \end{array} \tag{20}$$

Note that these functions always exist, because K_1 and K_2 are rigid transformations, and thus invertible. Multiplying ϵ_1 and ϵ_2:

$$\epsilon_1(\boldsymbol{\zeta}) \cdot \epsilon_2(\boldsymbol{\mu}) = K_1(\boldsymbol{\zeta};\tilde{\boldsymbol{\mu}})^{-1} \cdot N_1(\boldsymbol{\zeta}) \cdot N_2(\boldsymbol{\mu}) \cdot K_2(\boldsymbol{\mu};\tilde{\boldsymbol{\mu}})^{-1},$$

using the composition equation (13) that N_1 and N_2 are assumed to satisfy,

$$\epsilon_1(\boldsymbol{\zeta}) \cdot \epsilon_2(\boldsymbol{\mu}) = K_1(\boldsymbol{\zeta};\tilde{\boldsymbol{\mu}})^{-1} \cdot K(\boldsymbol{\zeta},\boldsymbol{\mu}) \cdot K_2(\boldsymbol{\mu};\tilde{\boldsymbol{\mu}})^{-1},$$

and applying (4) and (2),

$$\epsilon_1(\boldsymbol{\zeta}) \cdot \epsilon_2(\boldsymbol{\mu}) = K_1(\boldsymbol{\zeta};\tilde{\boldsymbol{\mu}})^{-1} \cdot K_1(\boldsymbol{\zeta};\tilde{\boldsymbol{\mu}}),$$

we obtain:

$$\epsilon_1(\boldsymbol{\zeta}) \cdot \epsilon_2(\boldsymbol{\mu}) = I. \tag{21}$$

Since ϵ_1 and ϵ_2 are functions dependent on different variables, they cannot cancel out the variable dependency of each other by means of multiplication. The only way of satisfying (21) is having $\epsilon_1 = C^{-1}$ and $\epsilon_2 = C$ for some constant C. Substituting ϵ_1 and ϵ_2 by these constants in (20),

$$\begin{array}{rcl} C^{-1} & = & K_1(\boldsymbol{\zeta};\tilde{\boldsymbol{\mu}})^{-1} \cdot N_1(\boldsymbol{\zeta}) \\ C & = & N_2(\boldsymbol{\mu}) \cdot K_2(\boldsymbol{\mu};\tilde{\boldsymbol{\mu}})^{-1}, \end{array} \tag{22}$$

yielding that (17) is the only form that N_1 and N_2 can exhibit.

We have demonstrated that all possible decompositions build by multiplying two functions of the two subsets of joints are the same up to a constant. This is the case for functions K_1 and K_2 with different reference values, $\tilde{\boldsymbol{\mu}}$ and $\tilde{\boldsymbol{\mu}}'$:

$$\begin{array}{rcl} K_1(\boldsymbol{\zeta};\tilde{\boldsymbol{\mu}}) & = & K_1(\boldsymbol{\zeta};\tilde{\boldsymbol{\mu}}') \cdot C_{\tilde{\boldsymbol{\mu}}'}^{-1} \cdot C_{\tilde{\boldsymbol{\mu}}} \\ K_2(\boldsymbol{\mu};\tilde{\boldsymbol{\mu}}) & = & C_{\tilde{\boldsymbol{\mu}}}^{-1} \cdot C_{\tilde{\boldsymbol{\mu}}'} \cdot K_2(\boldsymbol{\mu};\tilde{\boldsymbol{\mu}}'). \end{array} \tag{23}$$

These relations are deduced from (3) and (7), respectively.

The result applies also to the alternative decomposition mentioned in Section II,

$$K(\boldsymbol{\zeta},\boldsymbol{\mu}) = L_2(\boldsymbol{\zeta}) \cdot L_1(\boldsymbol{\mu}),$$

for which it can be shown that

$$\begin{array}{rcl} L_2(\boldsymbol{\zeta}) & = & K_1(\boldsymbol{\zeta}) \cdot C \\ \text{and} \qquad L_1(\boldsymbol{\mu})^{-1} & = & C^{-1} \cdot K_2(\boldsymbol{\mu}). \end{array}$$

B. Deformations learnable with only one function

When the learning of N_2 is removed from Algorithm 3 (i.e., only N_1 is learned), it is still possible to adapt the composition to certain deformations. Let K' denote the new deformed kinematics and let K_1' and K_2' be the new component functions for the chosen $\tilde{\boldsymbol{\mu}}$. All deformations for which there exists a constant C satisfying

$$K'(\boldsymbol{\zeta},\boldsymbol{\mu}) \cdot N_2(\boldsymbol{\mu})^{-1} = K_1'(\boldsymbol{\zeta}) \cdot C \tag{24}$$

can be learned by N_1 alone. The left side of the equation is the function learned by N_1 in Algorithm 3 when N_2 is fixed. The right side is the form of the functions that N_1 is allowed to encode to yield a valid composition. If N_2 is assumed to be correctly learned before the deformation (i.e., $N_2(\boldsymbol{\mu}) = C_{old} \cdot K_2(\boldsymbol{\mu})$), a simpler condition can be stated:

$$K_2'(\boldsymbol{\mu}) = C \cdot K_2(\boldsymbol{\mu}) \tag{25}$$

In fact, using the assumption, it is easy to prove that (25) implies (24):

$$\begin{aligned} K'(\boldsymbol{\zeta},\boldsymbol{\mu}) \cdot N_2(\boldsymbol{\mu})^{-1} &= K'(\boldsymbol{\zeta},\boldsymbol{\mu}) \cdot (C_{old} \cdot K_2(\boldsymbol{\mu}))^{-1} \\ &= K'(\boldsymbol{\zeta},\boldsymbol{\mu}) \cdot K_2(\boldsymbol{\mu})^{-1} \cdot C_{old}^{-1} \\ &= K'(\boldsymbol{\zeta},\boldsymbol{\mu}) \cdot (C^{-1} \cdot K_2'(\boldsymbol{\mu}))^{-1} \cdot C_{old}^{-1} \\ &= K'(\boldsymbol{\zeta},\boldsymbol{\mu}) \cdot K_2'(\boldsymbol{\mu})^{-1} \cdot C \cdot C_{old}^{-1} \\ &= K_1'(\boldsymbol{\zeta}) \cdot C \cdot C_{old}^{-1}. \end{aligned}$$

The condition equivalent to (25) for the case of learning N_2 alone is that

$$K_1'(\boldsymbol{\zeta}) = K_1(\boldsymbol{\zeta}) \cdot C \tag{26}$$

for some C.

Now it is easy to see that if the kinematics of the robot undergoes a deformation equivalent to a linear transformation, that is,

$$K'(\boldsymbol{\zeta},\boldsymbol{\mu}) = K(\boldsymbol{\zeta},\boldsymbol{\mu}) \cdot P,$$

the system can be quickly adapted by learning N_2 alone. A linear transformation includes rigid transformations, as those involved in adaptation to a tool. And also includes some camera miscalibrations leading for example to a scaling of the sensor data. In effect, since

$$\begin{aligned} K_1'(\boldsymbol{\zeta}) &= K'(\boldsymbol{\zeta},\tilde{\boldsymbol{\mu}}) = K(\boldsymbol{\zeta},\tilde{\boldsymbol{\mu}}) \cdot P & (27) \\ &= K_1(\boldsymbol{\zeta}) \cdot P, & (28) \end{aligned}$$

condition (26) is fulfilled. Instead, learning N_1 alone does not work. Using (6),

$$\begin{aligned} K_2'(\boldsymbol{\mu}) &= K'(\boldsymbol{\zeta},\boldsymbol{\mu})^{-1} \cdot K'(\boldsymbol{\zeta},\tilde{\boldsymbol{\mu}}) & (29) \\ &= (K(\boldsymbol{\zeta},\tilde{\boldsymbol{\mu}}) \cdot P)^{-1} \cdot K(\boldsymbol{\zeta},\boldsymbol{\mu}) \cdot P & (30) \\ &= P^{-1} \cdot K(\boldsymbol{\zeta},\tilde{\boldsymbol{\mu}})^{-1} \cdot K(\boldsymbol{\zeta},\boldsymbol{\mu})\ P, & (31) \end{aligned}$$

and using again (6),

$$K_2'(\boldsymbol{\mu}) = P^{-1} \cdot K_2(\boldsymbol{\mu}) \cdot P. \tag{32}$$

There is no possibility to satisfy (25), except for the case when $P = I$.

REFERENCES

[1] Y. Zhao and C. C. Cheah, "Neural network control of multifingered robot hands using visual feedback," *IEEE Transactions on Neural Networks*, vol. 20, no. 5, pp. 758 –767, May 2009.

[2] J. Walter and H. Ritter, "Rapid learning with parametrized self-organizing maps," *Neurocomputing*, vol. 12, no. 2-3, pp. 131 – 153, 1996.

[3] S. Vijayakumar, A. D'Souza, and S. Schaal, "Incremental online learning in high dimensions," *Neural Computation*, vol. 17, pp. 2602–2634, 2005.

[4] V. R. de Angulo and C. Torras, "Speeding up the learning of robot kinematics through function decomposition," *IEEE Transactions on Neural Networks*, vol. 16, no. 6, pp. 1504–1512, 2005.

[5] G. Metta, G. Sandini, G. S, and L. Natale, "Sensorimotor interaction in a developing robot," in *In First International Workshop on Epigenetic Robotics: Modeling Cognitive Development in Robotic Systems*. Lund University Press, 2001, pp. 18–19.

[6] S. Ulbrich, V. Ruiz, T. Asfour, C. Torras, and R. Dillmann, "Rapid learning of humanoid body schemas with kinematic bézier maps," in *Proc. IEEE-RAS International Conference on Humanoid Robots-09*, Paris, France, Dec. 2009, pp. 431–438.

[7] V. R. de Angulo and C. Torras, "Learning inverse kinematics: Reduced sampling through decomposition into virtual robots," *IEEE Transactions on Systems, Man and Cybernetics - part B*, vol. 38, no. 6, pp. 1571–1577, 2008.

[8] D. Whitney, "Resolved motion rate control of manipulators and human prostheses," *IEEE Transactions on Man-Machine Systems*, vol. 10, no. 2, pp. 47–53, June 1969.

[9] A. Ligeois, "Automatic supervisory control of the configuration and behavior of multibody mechanisms," *IEEE Transactions on Systems, Man and Cybernetics*, vol. 7, no. 12, pp. 868 –871, Dec. 1977.

[10] L. Li, W. Gruver, Q. Zhang, and Z. Yang, "Kinematic control of redundant robots and the motion optimizability measure," *IEEE Transactions on Systems, Man, and Cybernetics, Part B: Cybernetics*, vol. 31, no. 1, pp. 155 –160, Feb. 2001.

[11] Y. Xia, G. Feng, and J. Wang, "A primal-dual neural network for online resolving constrained kinematic redundancy in robot motion control," *IEEE Transactions on Systems, Man, and Cybernetics, Part B: Cybernetics*, vol. 35, no. 1, pp. 54 –64, Feb. 2005.

[12] M. Hersch, E. Sauser, and A. Billard, "Online learning of the body schema," *International Journal of Humanoid Robotics*, vol. 5, no. 2, pp. 161–181, 2008.

[13] R. Martinez-Cantin, M. Lopes, and L. Montesano, "Body schema acquisition through active learning," in *Proc. of the IEEE Int. Conf. on Robotics & Automation*, 2010.

[14] G. Sun and B. Scassellati, "Reaching through learned forward model," in *IEEE-RAS International Conference on Humanoid Robots-04*, vol. 1, Nov. 2004, pp. 93–112.

[15] M. Rolf, J. Steil, and M. Gienger, "Goal babbling permits direct learning of inverse kinematics," *IEEE Transactions on Autonomous Mental Development*, vol. PP, no. 99, pp. 1 –1, 2010.

[16] Y. Zhang and S. Ge, "Design and analysis of a general recurrent neural network model for time-varying matrix inversion," *IEEE Transactions on Neural Networks*, vol. 16, no. 6, pp. 1477 –1490, Nov. 2005.